

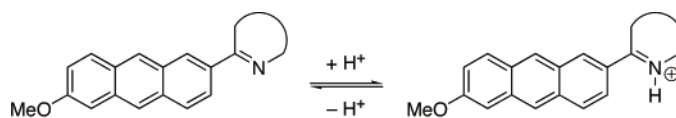
Anthryl-Substituted Heterocycles as Acid-Sensitive Fluorescence Probes

Heiko Ihmels,^{*,†} Andreas Meiswinkel,[‡] Christian J. Mohrschladt,[‡] Daniela Otto,[†]
Michael Waidelich,[†] Michael Towler,[§] Rick White,[§] Martin Albrecht,^{||} and
Alexander Schnurpfeil^{||,⊥}

Institut für Organische Chemie, Universität Siegen, Adolf-Reichwein-Str., D-57068 Siegen, Germany, Institut für Organische Chemie, Universität Würzburg, Am Hubland, D-97074 Würzburg, Germany, Department of Chemistry, Sam Houston State University, Huntsville, Texas 77341, and Institut für Physikalische und Theoretische Chemie, Universität Siegen, Adolf-Reichwein-Str., D-57068 Siegen, Germany

ihmels@chemie.uni-siegen.de

Received December 7, 2004



Change of emission wavelength
upon protonation:



Four pH-sensitive fluorescence probes are presented which consist of an anthracene fluorophore and a π -conjugated oxazoline, benzoxazole, or pyridine substituent. The protonation of the heterocycles increases their acceptor properties and results in significant red-shifts of the absorption and emission maxima of the anthracene chromophore. The comparison between 2-[2'-(6'-methoxyanthryl)]-4,4-dimethyl-2-oxazoline and 2-[2'-(anthryl)]-4,4-dimethyl-2-oxazoline reveals that the donor-acceptor substitution pattern of the fluorophore is not required to achieve a red shift upon protonation. The benzoxazole and pyridine substituents offer a particular advantage due to their persistence under acidic conditions. Thus, these compounds may be used as efficient pH-sensitive fluorescence switches. Nevertheless, the switching of benzoxazole **2c** requires relatively strong acidic conditions. The anthrylpyridinium exhibits a red-shifted emission in chloroform; however, it is nonfluorescent in aqueous or alcoholic solution. Although the oxazoline is not persistent under permanent acidic conditions, this heterocycle may be useful as a substituent in fluorescence indicators since it may be used to detect acid concentrations of 10^{-4} – 10^{-5} M, which are close to the biologically relevant range.

Introduction

Fluorescence spectroscopy has developed to one of the most important tools in analytical biology and medicine.¹ In particular, the high sensitivity of this method (even down to the single molecule)² is useful for the detection of analytes at low concentrations. Along these lines,

organic fluorophores exhibit a high potential to be part of fluorescence probes, since they offer the possibility to connect a fluorophore directly with a particularly designed functionality whose interaction with the analyte may have a significant influence on the emission properties such as emission intensity, wavelength, or lifetime. A survey of known fluorescence probes and switches, however, reveals that in the majority of systems the fluorescence intensity, i.e., the decrease or increase of emission quantum yield, is used to monitor the interactions with an external stimulus or analyte. Especially in the case of fluorescence quenching, this process is not

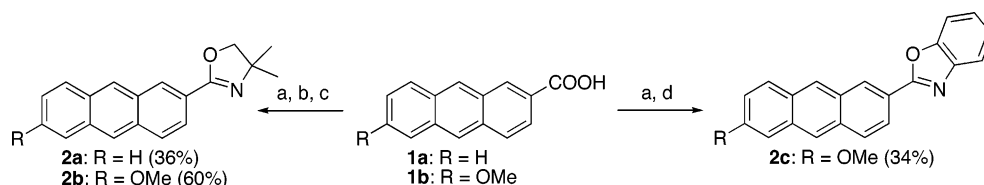
[†] Institut für Organische Chemie, Universität Siegen.

[‡] Institut für Organische Chemie, Universität Würzburg.

[§] Department of Chemistry, Sam Houston State University.

^{||} Institut für Physikalische und Theoretische Chemie, Universität Siegen.

[⊥] Present address: Institut für Theoretische Chemie, Universität Köln, Greinstr. 4, D-50939 Köln, Germany.

SCHEME 1^a

^a Key: (a) CO_2Cl_2 , reflux, 18 h; (b) 2-amino-2-methylpropanol, CH_2Cl_2 , rt, 2 h; (c) SOCl_2 , reflux 2 h; (d) 2-aminophenol, pyridine, 100 °C, 1 h, then 200 °C, 30 min.

very selective, since quenching may also be caused by other external factors. Therefore, fluorescence probes are desirable whose emission wavelength changes significantly in the presence of an analyte—as realized in fluorescent ED- π -EA systems. In most donor–acceptor-substituted fluorescence probes, the protonation or complexation of donor substituents leads to a decrease of their donor ability and to a corresponding blue shift of the absorption and emission maxima. This concept is very often realized with amino functionalities or crown and aza-crown substituents as donor moiety in a donor–acceptor-substituted chromophore.^{1c–e} In contrast, examples for complementary fluorescence probes and switches are rather rare, in which the modification of acceptor functionalities leads to a red-shift of the absorption and emission maxima,³ presumably because there are only few acceptor functionalities which offer the appropriate properties. Some examples are known in which a heterocycle with a CN double bond is used as tunable acceptor moiety, but to the best of our knowledge a systematic investigation has not been performed.^{3c–f} It may also be noted that fluorescence probes are very often used successfully to detect metal cations or inorganic and organic anions; however, the number of efficient proton-sensitive fluorescence probes is comparably small.⁴ In preliminary work, we have shown that the protonation of the anthryloxazoline **2b** results in a significant red

shift of its emission from 444 to 540 nm.⁵ In this paper, we present our studies on the scope and limits of this probe system on the basis of alkaline anthryl-substituted heterocycles.

Results

Synthesis. The anthryl-substituted oxazolines **2a** and **2b** as well as the benzoxazole **2c** were synthesized according to standard procedures (Scheme 1), starting from anthracene-2-carboxylic acid (**1a**) or 6-methoxyanthracene-2-carboxylic acid (**1b**).⁶ Thus, the transformation of carboxylic acids **1a** or **1b** to the corresponding acid chlorides, reaction with 2-methyl-2-aminobutanol, and subsequent cyclization with thionyl chloride gave the oxazolines **2a** and **2b** in 36% and 60% yield. The benzoxazole **2c** was obtained in rather low yield (34%) by the reaction of the acid chloride with 2-aminophenol (Scheme 1). The pyridyl-substituted anthracene **7** was synthesized from 2-(4'-methoxyphenyl)-4,4-dimethyl-2-oxazoline (**3**),⁷ which was ortho-lithiated with *n*-BuLi followed by the addition of 4-(2'-pyridyl)benzaldehyde to yield the diarylmethanol derivative **4** quantitatively. The latter was treated with *p*-toluenesulfonic acid to give the phthalide **5** in 62% yield (Scheme 2). Reduction with zinc dust in acetic acid gave the benzoic acid derivative **6**, which was cyclized with methanesulfonic acid and subsequently reduced to yield the anthracene **7**. Unfortunately, the cyclization–reduction sequence from **6** to **7** proceeds in low yields (21% over both steps), and attempts to optimize the reaction conditions did not lead to higher yields. All new compounds were characterized by ¹H and ¹³C NMR spectroscopy, mass spectrometry, and elemental analysis or high-resolution mass spectrometry.

Photophysical Properties. The absorption properties of compounds **2a–c** and **7** are characteristic of substituted anthracene derivatives (Table 1, data of **2a** not shown); i.e., short-wavelength absorption bands (S_0 – S_3 transition)⁸ appear between 250 and 300 nm and long-wavelength absorption bands (p band: S_0 – S_1 transition) between 300 and 430 nm. Moreover, the absorption bands of the donor–acceptor system **2b** are shifted ca. 30 nm to longer wavelength as compared to **2a** due to the presence of the additional donor substituent which is linearly conjugated with the acceptor moiety. In all cases, there is no long-wavelength absorption, which reveals the absence of an ICT absorption. For all compounds, the absorption properties are almost independent from the solvent (Table 1).

(1) (a) *Optical Sensors*; Wolfbeis, O. S., Ed.; Springer-Verlag: Heidelberg, 2004. (b) Mohr, G. *J. Chem. Eur. J.* **2004**, *10*, 1082–1090. (c) Pu, L. *Chem. Rev.* **2004**, *104*, 1687. (d) Martinez-Manez, R.; Sancenon, F. *Chem. Rev.* **2003**, *103*, 4419. (e) Wiskur, S. L.; Ait-Haddou, H.; Anslyn, E. V.; Lavigne, J. *J. Acc. Chem. Res.* **2001**, *34*, 963. (f) *Chemosensors of Ion and Molecular Recognition*; Desvergne, J.-P., Czarnik, A. W., Eds.; Kluwer Academic Press: Dordrecht, The Netherlands, 1997. (g) de Silva, A. P. H.; Gunaratne, Q.; Gunlaugsson, T.; Huxley, A. J. M.; McCoy, C. P.; Rademacher, J. T.; Rice, T. E. *Chem. Rev.* **1997**, *97*, 1515. (h) *Fluorescent Chemosensors for Ion and Molecule Recognition*; Czarnik, A. W., Ed.; ACS Symposium Series No. 538; American Chemical Society: Washington DC, 1993. (i) Valeur, B. In *Topics in Fluorescence Spectroscopy, Vol. 4: Probe Design and Chemical Sensing*; Lakowicz, J. R., Ed.; Plenum Press: New York, 1994; Chapter 2.

(2) (a) Sauer, M. *Angew. Chem.* **2003**, *115*, 1834; *Angew. Chem., Int. Ed. Engl.* **2003**, *42*, 1790. (b) Ambrose, W. P.; Goodwin, P. M.; Jett, J. H.; van Orden, A.; Werner, J. H.; Keller, R. A. *Chem. Rev.* **1999**, *99*, 2929. (c) Ha, T.; Chemla, D. S.; Enderle, T.; Weiss, S. *Bioimaging* **1997**, *55*, 99.

(3) (a) Bourson, J.; Pouget, J.; Valeur, B. *J. Phys. Chem.* **1993**, *97*, 4552. (b) Dix, J. P.; Vögtle, F. *Chem. Ber.* **1981**, *114*, 638. (c) Jones, G., II; Jiminez, J. A. C. *J. Photochem. Photobiol. B: Biology* **2001**, *65*, 5. (d) Fayed, T. A. *J. Photochem. Photobiol. A: Chemistry* **1999**, *121*, 17. (e) Corrent, S.; Hahn, P.; Pohlars, G.; Connolly, T. J.; Scaiano, J. C.; Fornes, V.; Garcia, H. *J. Phys. Chem. B* **1998**, *102*, 5852. (f) Wolfbeis, O. S.; Marhold, H. *Chem. Ber.* **1985**, *118*, 3664.

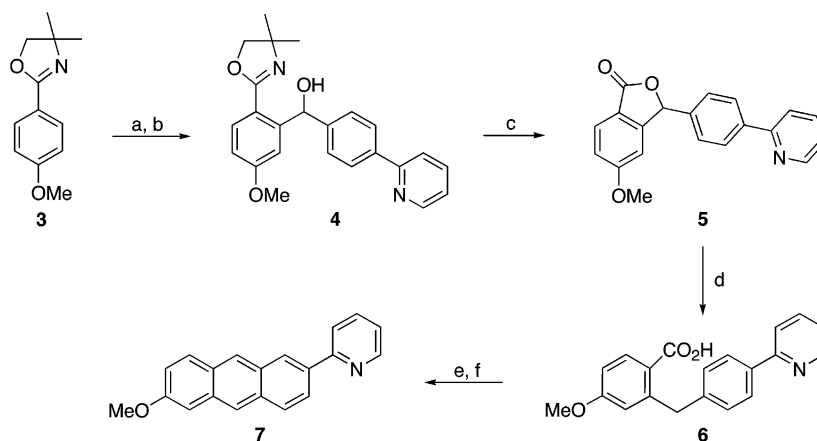
(4) For recent examples see: (a) Charier, S.; Ruel, O.; Baudin, J.-B.; Alcor, D.; Allemand, J.-F.; Meglio, A.; Jullien, L. *Angew. Chem.* **2004**, *43*, 4785; *Angew. Chem., Int. Ed. Engl.* **2004**, *116*, 4889. (b) Cui, D.; Quian, X.; Liu, F.; Zhang, R. *Org. Lett.* **2004**, *6*, 2757. (c) Diwu, Z.; Chen, C.-S.; Zhang, C.; Klauert, D. H.; Haugland, R. P. *Chem. Biol.* **1999**, *6*, 411. (d) Kermis, H. R.; Kostov, Y.; Harms, P.; Rao, G. *Biotech. Prog.* **2002**, *18*, 1047. (e) Garreis, T.; Huber, C.; Wolfbeis, O. S.; Daub, J. *J. Chem. Soc., Chem. Commun.* **1997**, 1717.

(5) Ihmels, H.; Meiswinkel, A.; Mohrschladt, C. *J. Org. Lett.* **2000**, *2*, 2865.

(6) Ihmels, H. *Eur. J. Org. Chem.* **1999**, 1595.

(7) Mohan, R.; Katzenellenbogen, J. A. *J. Org. Chem.* **1984**, *49*, 1238.

(8) Dick, B.; Hohlneicher, G. *Chem. Phys. Lett.* **1981**, *83*, 615.

SCHEME 2^a

^a Key: (a) *n*-BuLi (1.6 M in hexane), Et₂O, 0 °C, 4 h; (b) 4-(2'-pyridyl)benzaldehyde; Et₂O, rt, 16 h (97% over both steps); (c) *p*-TsOH, toluene, reflux, 2.5 h (62%); (d) Zn, CH₃COOH, reflux, 24 h (75%); (e) CH₃SO₃H, 90 °C, 4 h; (f) NaBH₄, 2-PrOH, reflux, 4 d (21% over both steps).

TABLE 1. Absorption and Emission Data (λ in nm) of the Anthracene Derivatives **2b, **2c**, and **7** (Solvents in Order of Decreasing $E_T(30)$ Value)**

solvent	2b			2c			7		
	λ_{abs}^a	$\log \epsilon$	$\lambda_{\text{fl}}^b (\phi_{\text{fl}})^c$	λ_{abs}^a	$\log \epsilon$	$\lambda_{\text{fl}}^b (\phi_{\text{fl}})^c$	λ_{abs}^a	$\log \epsilon$	$\lambda_{\text{fl}}^d (\phi_{\text{fl}})^e$
<i>c</i> -C ₆ H ₁₂	393	3.78	421 ^e (0.30)	404	4.05	433 ^f (0.49)	398	3.73	426 ^g (0.26)
benzene	396	3.66	430	407	3.99	442 (0.43)	402	3.72	434 (0.28)
CH ₂ Cl ₂	395	3.64	438 (0.49)	406	3.97	452 (0.44)	401	3.69	438 (0.26)
1-BuCN	394	3.63	435 (0.42)	405	3.97	453 (0.48)			
DMF	396	3.64	441 (0.50)	407	3.97	458 (0.45)	401	3.65	441 (0.35)
DMSO	397	3.64	444 (0.58)	409	3.97	461 (0.43)	404	3.70	444 (0.34)
MeCN	392	3.59	439 (0.42)	404	3.95	456 (0.45)	398	3.67	438 (0.29)
MeOH	395	3.61	444 (0.48)	403	4.01	462 (0.43)	398	3.70	440 (0.28)

^a Maximum at lowest energy; $c = 10^{-4}$ M. ^b Emission maximum; $c = 10^{-5}$ M, $\lambda_{\text{ex}} = 390$ nm. ^c Relative to quinine sulfate in 1 N H₂SO₄. ^d Emission maximum, $c = 10^{-5}$ M, $\lambda_{\text{ex}} = 380$ nm. ^e Additional emission band at $\lambda = 442$. ^f Additional emission bands at $\lambda = 456$ nm. ^g Additional emission band at $\lambda = 408$ and 451 nm.

The emission spectra of compounds **2a–c** and **7** exhibit very broad, mostly structureless bands. In contrast to the absorption data, the emission properties of **2b**, **2c**, and **7** show a moderate dependence on the solvent properties. In general, a correlation of the emission wavelength with the solvent polarity was observed, as expressed by the empirical parameter $E_T(30)$.⁹ Thus, a red shift of the emission band results from an increasing solvent polarity. This effect is especially pronounced for benzoxazole **2c** (Figure 1) and leads to the conclusion that the dipole moment of the excited state is larger than the one of the ground state.¹⁰ Notably, emission data in methanol do not fit into the correlation, presumably because along with the dipole–dipole interactions between solvent and chromophore hydrogen bonding may have an influence on the emission properties in methanol.

Dependence of the Electronic Spectra on the Proton Concentration. Upon acidification of the oxa-

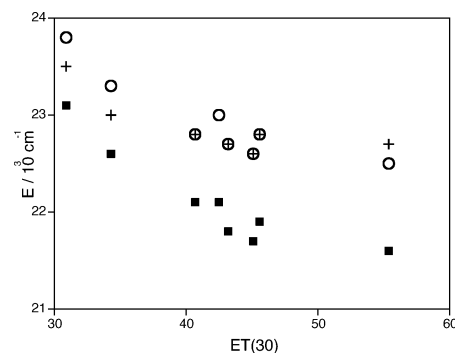


FIGURE 1. Correlation of the emission maxima (in cm^{-1}) of **2b** (O, $r^2 = 0.88$), **2c** (■, $r^2 = 0.94$), and **7** (+, $r^2 = 0.82$) with the solvent parameter $E_T(30)$ (for the r^2 values, methanol was excluded).

zolines **2a** and **2b** or pyridine **7** with hydrochloric acid in methanol solution, a remarkable shift of the absorption maximum was observed along with a significant loss of the absorption-band structure (Figures 2–4 and Table

(9) Reichardt, C. *Chem. Rev.* **1994**, *94*, 2319.

(10) Suppan, P.; Ghoneim, N. *Solvatochromism*; The Royal Society of Chemistry: London, 1997.

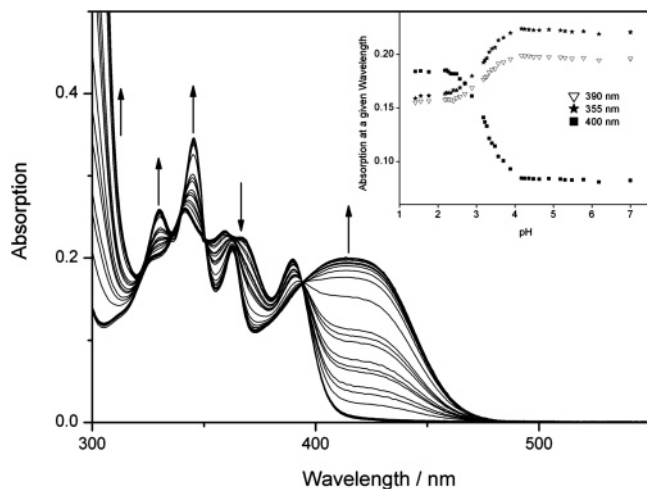


FIGURE 2. Spectrophotometric titration of **2a** (10^{-4} M in MeOH) with aqueous HCl; arrows indicate the development of band maxima during titration. Inset: change of absorption intensity at 355, 390, and 400 nm at varying acid concentrations.

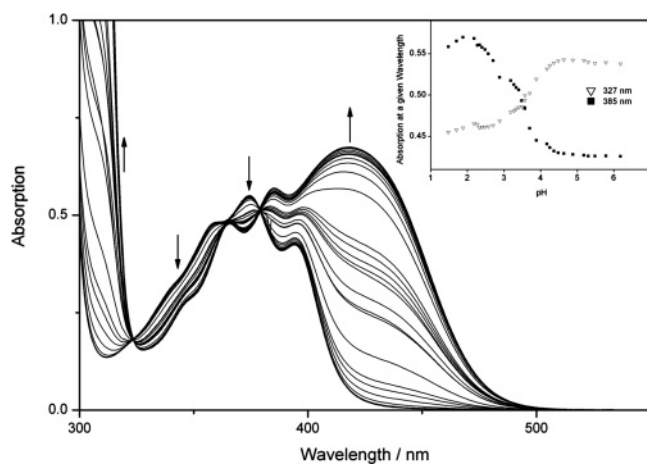


FIGURE 3. Spectrophotometric titration of **2b** (10^{-4} M in MeOH) with aqueous HCl; arrows indicate the development of band maxima during titration. Inset: change of absorption intensity at 372 and 385 nm at varying acid concentrations.

2, cf. Supporting Information for magnified Figures). In each case, a plot of the absorption at a fixed wavelength versus the proton concentration exhibits the characteristic features of a spectrophotometric acid–base titration. From these isotherms, the pK_a values of the conjugated acids were estimated to be 3.2 (**2a**), 3.5 (**2b**), and 2.7 (**7**) under these conditions (Table 2). The pK_a values of **2a–c** and **7** differ about 2–3 orders of magnitude from the ones reported for oxazoline, pyridine, and benzoxazole derivatives;^{3d,11} however, the latter have been determined in water, whereas the data reported herein were determined in methanol solutions, in which pK values are usually smaller than in water.¹² The excited-state pK_a , i.e., pK_a^* , were estimated from Förster-cycle calculations (Table 2). Thus, as usually observed for *N*-heterocycles,¹³ the protonated oxazolines **2a** and **2b** and the protonated pyridine

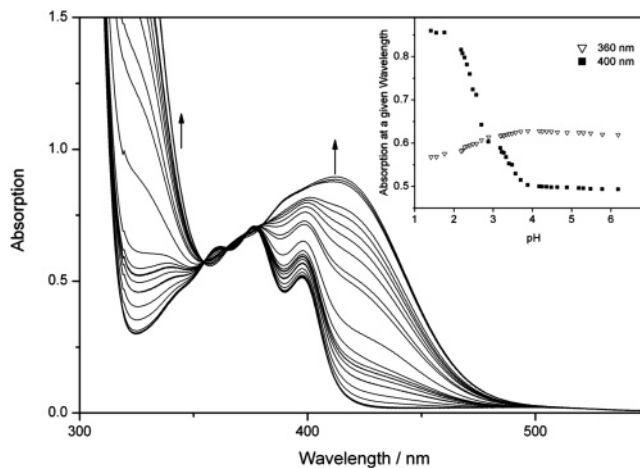


FIGURE 4. Spectrophotometric titration of **7** (10^{-4} M in MeOH) with aqueous HCl; arrows indicate the development of band maxima during titration. Inset: change of absorption intensity at 360 and 400 nm at varying acid concentrations.

TABLE 2. Emission Data and pK_a Values from Unprotonated and Protonated Anthracene Derivatives **2a–c** and **7**

	λ_{fl} (no H^+) (nm)	λ_{fl} ($+H^+$) (nm)	pK_a^b	pK_a^*c
2a ^a	426 ^d	517 ^d	3.2	10.2
2b ^a	450 ^e	544 ^e	3.5	10.1
2c ^a	469 ^e	567 ^e	<1	
7 ^a	443 ^f	540 ^f	2.7 ^g	9.1

^a $c = 10^{-5}$ M. ^b Determined from spectrophotometric titration in MeOH with aq HCl, error ± 0.1 . ^c Calculated according to Förster cycle: $\Delta pK = 0.00209 [\bar{\nu}(\text{base}) - \bar{\nu}(\text{base-}H^+)]/\text{cm}^{-1}$. ^d $\lambda_{ex} = 363$ nm. ^e $\lambda_{ex} = 380$ nm. ^f $\lambda_{ex} = 370$ nm. ^g Same pK in $CHCl_3$ with trifluoroacetic acid.

7 are significantly less acidic in the excited state as compared to the ground state (ΔpK_a of ca. 7).

In contrast, spectrophotometric titrations of acid to benzoxazole **2c** have no significant influence on the absorption spectrum at moderate acid concentration ($>10^{-1}$ M). Nevertheless, at larger acid concentrations, a decrease of the long-wavelength absorption band was observed along with the formation of a shoulder from 430 to 500 nm (Figure 5).

The emission maximum of oxazolines **2a** and **2b** in methanol solution was significantly quenched upon addition of acid, and a new maximum appeared at $\lambda = 517$ nm and $\lambda = 544$ nm, respectively (Figures 6 and 7). Further acidification led to a decrease of the short-wavelength fluorescence and to an increase of the red-shifted emission. It was also shown exemplarily for **2b** that the same effect may be achieved in water solution (Figure 7B); however, the low solubility of the anthracene derivative requires lower concentrations (10^{-6} M). Notably, the change of emission color may be followed by the naked eye in each case (Figure 8). On neutralization of the solution, the initial emission spectrum of anthracene **2b** was regained. In principle, the benzoxazole **2c** exhibits the same emission behavior as **2a** and **2b** upon spectrofluorimetric titration with hydrochloric acid (Figure 9);

(11) Albert, A. *Heterocyclic Chemistry*, 2nd ed.; Athlone Press: London, 1968; Chapter 13.

(12) Reichardt, C. *Solvents and Solvent Effects on Organic Chemistry*, 3rd ed.; Wiley-VCH: Weinheim, 2003; Chapter 4.2.

(13) Ireland, J. F.; Wyatt, P. A. H. *Adv. Phys. Org. Chem.* **1976**, *12*, 131.

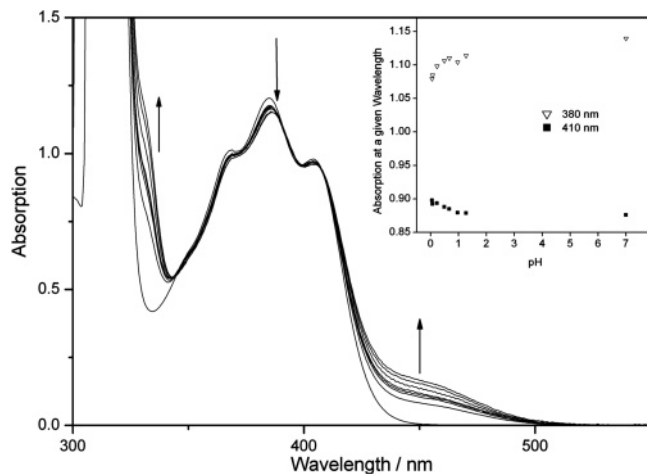


FIGURE 5. Spectrophotometric titration of **2c** (10^{-4} M in MeOH) with aqueous HCl; arrows indicate the development of band maxima during titration. Inset: change of absorption intensity at 380 and 410 nm at varying acid concentrations.

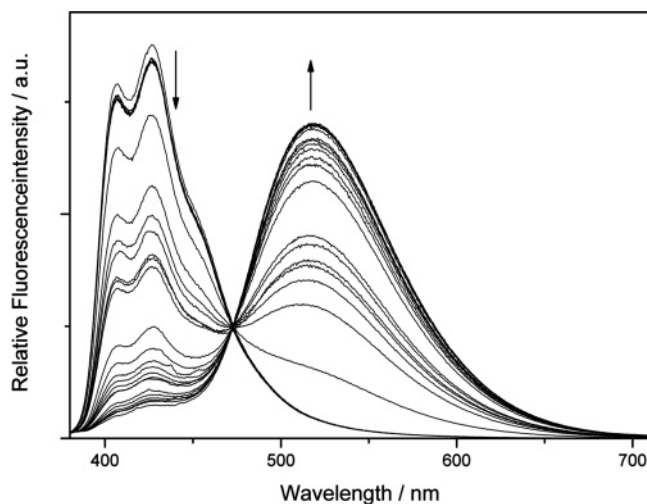


FIGURE 6. Spectrofluorimetric titration of **2a** (10^{-5} M in MeOH) with aqueous HCl; arrows indicate the development of band maxima during titration; $\lambda_{\text{ex}} = 363$ nm. Before titration: $c(\text{HCl}) = 0$ M. Titration end: $c(\text{HCl}) = 3.2 \times 10^{-2}$ M.

however, the formation of a new red-shifted emission band requires significantly higher acid concentrations.

In methanol solution, the fluorescence intensity of the anthryl-pyridine **7** was significantly quenched upon addition of aqueous hydrochloric acid (Figure 10A), but in contrast to observations with the oxazolines **2a** and **2b**, only a very weak red-shifted emission maximum was observed. Nevertheless, the addition of trichloroacetic acid to **7** in chloroform solution led to a quenching of the emission maximum along with the formation of a new band at $\lambda = 540$ nm (Figure 10B).

Discussion

The donor–acceptor interplay in compounds **2a–c** and **7** appears to be weak as deduced from their absorption and emission spectra, i.e., no ICT absorption bands and only a moderate solvatochromism of the emission properties have been observed. Nevertheless, the protonation

of the heterocyclic moiety of anthracenes **2a**, **2b**, and **7** transforms them in stronger acceptor functionalities and results in a significant red shift of the absorption band which is assigned to an ICT absorption. The oxazolines **2a** and **2b** as well as the pyridine **7** are protonated at moderate acid concentrations, whereas the aromatic benzoxazole **2c** requires significantly higher acid concentrations for protonation. These observations are in good agreement with the reported pK_a data for parent compounds and derivatives thereof.^{3d,11} Preliminary interpretations of absorption and emission data with the protonated anthryloxazoline **2b** suggested that the resulting “oxazolinium substituent” has a higher π -acceptor strength than the oxazoline, so that a stronger donor–acceptor interplay with the conjugated methoxy functionality is established, along with the corresponding red-shifted absorption and emission maxima relative to the ones of nonprotonated **2b**. However, the same effect was observed for the oxazoline **2a**, which does not have a conjugated methoxy group attached to the anthracene fluorophore. This somewhat surprising result reveals that the donor substituent in the 6 position, and thus a conjugated donor–acceptor system in general, is not necessarily required to achieve the drastic red shift upon protonation. Moreover, this observation is in agreement with studies which show that anthracene moieties may act as efficient electron donors in photoinduced charge-transfer processes.¹⁴

The proposed qualitative explanations of the photophysical properties of compounds **2a** and **2b** along with the ones of their protonated forms were supported by density functional theory (DFT) ab initio calculations on slightly varied systems **2a'** and **2b'**. To keep the computational effort feasible, the two methyl substituents on the oxazoline moiety were omitted. Note that the purpose of the calculations was not to simulate the experimental data including all specific and nonspecific interactions with the respective solvent but to analyze the observed trends in the absorption and emission spectra. In each calculation, the structure was first obtained from a DFT geometry optimization employing the RI-DFT method with the B-P86 functional and a cc-pVTZ basis set using the program package TURBOMOL.¹⁵ Subsequently, the difference between electron affinity and ionization potential was calculated employing GAUSSIAN03¹⁶ with a B3LYP functional in a 6-311+G** basis set. The resulting difference was used to estimate the HOMO–LUMO gap and the corresponding absorption (and emission) wavelength. Thus, for **2a'** and **2b'** a HOMO–LUMO gap of 364 and 380 nm was calculated, respectively, whereas the corresponding protonated forms exhibit HOMO–LUMO gaps of 477 or 502 nm. These theoretical data confirm the experimental trend, i.e., that the protonated anthryloxazolines exhibit considerably red-shifted absorption and emission maxima compared to the unprotonated molecules (see, e.g., the emission data:

(14) See, e.g.: Hirsch, T.; Port, H.; Wolf, H. C.; Miehlich, B.; Effenberger, F. *J. Phys. Chem. B* **1997**, *101*, 4525.

(15) TURBOMOLE Version 5, Ahlrichs, R.; M. Bär, M.; Baron, H.-P.; Bauernschmitt, R.; Böcker, S.; Furche, F.; Haase, F.; Häser, M.; Horn, H.; Hättig, C.; Huber, C.; Huniar, U.; Kattaneck, M.; Köhn, A.; Kölmel, C.; Kollwitz, M.; May, K.; Ochsenfeld, C.; Öhm, H.; Schäfer, A.; Schneider, U.; Sierka, M.; Treutler, O.; Unterreiner, B.; Arnim, M. V.; Weigend, F.; Weiss, P.; Weiss, H. Institut f. Physikalische Chemie, Universität Karlsruhe, Kaiserstr. 12, D-76128 Karlsruhe, 1998.

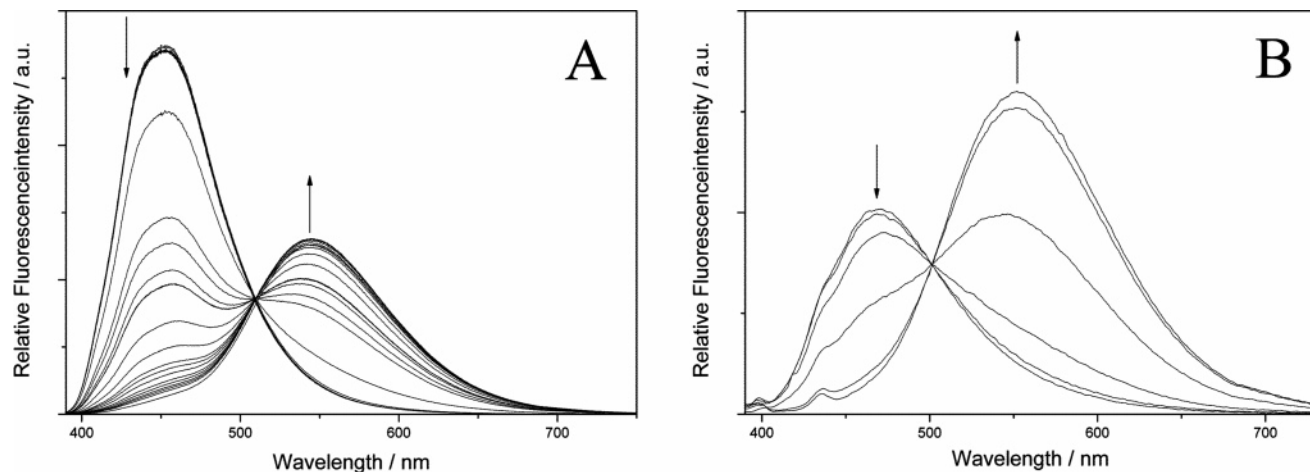


FIGURE 7. (A) Spectrofluorimetric titration of **2b** (10^{-5} M in MeOH) with aqueous HCl; arrows indicate the development of band maxima during titration. Before titration: $c(\text{HCl}) = 0$ M. Titration end: $c(\text{HCl}) = 3.2 \times 10^{-2}$ M. (B) Fluorescence spectra of **2b** (10^{-6} M in Britton–Robinson buffer at pH 2, 3, 4, 5, 6, 7; cont. 1% DMSO); $\lambda_{\text{ex}} = 380$ nm; arrows indicate the development of band maxima upon decreasing pH.

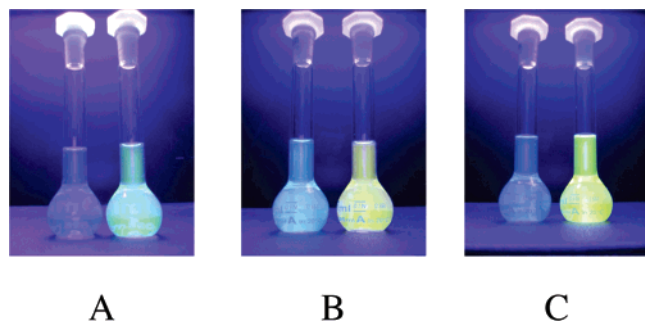


FIGURE 8. Pictures of unprotonated (left) and protonated (right) forms of **2a** (A), **2b** (B), and **7** (C), $\lambda_{\text{ex}} = 366$ nm. A and B: $c = 10^{-5}$ M in methanol. C: $c = 10^{-5}$ M in CHCl_3 .

2a': $\Delta\lambda = 103$ nm; **2b'**: $\Delta\lambda = 122$ nm). Furthermore, it can be seen that **2b'** is red-shifted with respect to its **2a'** counterpart by 16 nm from 364 to 380 nm, which is also in agreement with the experimental data.

To discuss the observed photophysical properties from the point of view of a simplified single electron orbital picture, the Kohn–Sham HOMO and LUMO orbitals for neutral and protonated **2a'** and **2b'** were used (Figure 11 and Figure 12). These orbitals reveal that in each case the LUMO has somewhat more weight on the oxazoline or the oxazolinium moiety, whereas in the HOMO most of the electron density is accumulated in the anthracene

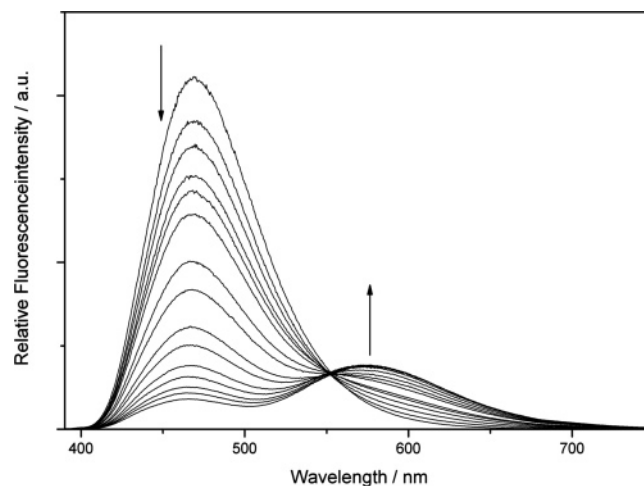


FIGURE 9. Spectrofluorimetric titration of **2c** (10^{-5} M in MeOH) with aqueous HCl; arrows indicate the development of band maxima during titration; $\lambda_{\text{ex}} = 380$ nm. Before titration: $c(\text{HCl}) = 0$ M. Titration end: $c(\text{HCl}) = 3.2 \times 10^{-1}$ M.

moiety. In addition, this effect is more significant for the protonated molecules. Moreover, the pictorial representation of orbital coefficients documents nicely the degree of charge transfer upon photoexcitation of the protonated anthryloxazolines, which leads to the significant red shift of the absorption and emission maxima as compared to the unprotonated molecule. Thus, the electron density in the HOMO, which is almost equally distributed all over the anthracene framework, is significantly shifted toward the oxazolinium moiety in the LUMO. Notably, this effect also takes place in **2a'**, which confirms our proposal that anthracene may act as a donor toward the protonated oxazoline substituent even when there is no additional π -conjugated donor substituent present. These results are in good agreement with theoretical studies on 3-styryl-substituted pyridine and pyridinium derivatives.¹⁷

(16) Gaussian 03, Revision B.04: Frisch, M. J.; Trucks, G. W.; Schlegel, H. B.; Scuseria, G. E.; Robb, M. A.; Cheeseman, J. R.; Montgomery, J. A., Jr.; Vreven, T.; Kudin, K. N.; Burant, J. C.; Millam, J. M.; Iyengar, S. S.; Tomasi, J.; Barone, V.; Mennucci, B.; Cossi, M.; Scalmani, G.; Rega, N.; Petersson, G. A.; Nakatsuji, H.; Hada, M.; Ehara, M.; Toyota, K.; Fukuda, R.; Hasegawa, J.; Ishida, M.; Nakajima, T.; Honda, Y.; Kitao, O.; Nakai, H.; Klene, M.; Li, X.; Knox, J. E.; Hratchian, H. P.; Cross, J. B.; Adamo, C.; Jaramillo, J.; Gomperts, R.; Stratmann, R. E.; Yazyev, O.; Austin, A. J.; Cammi, R.; Pomelli, C.; Ochterski, J. W.; Ayala, P. Y.; Morokuma, K.; Voth, G. A.; Salvador, P.; Dannenberg, J. J.; Zakrzewski, V. G.; Dapprich, S.; Daniels, A. D.; Strain, M. C.; Farkas, O.; Malick, D. K.; Rabuck, A. D.; Raghavachari, K.; Foresman, J. B.; Ortiz, J. V.; Cui, Q.; Baboul, A. G.; Clifford, S.; Cioslowski, J.; Stefanov, B. B.; Liu, G.; Liashenko, A.; Piskorz, P.; Komaromi, I.; Martin, R. L.; Fox, D. J.; Keith, T. Al-Laham, M. A.; Peng, C. Y.; Nanayakkara, A.; Challacombe, M.; Gill, P. M. W.; Johnson, B.; Chen, W.; Wong, M. W.; Gonzalez, C.; Pople, J. A. Gaussian, Inc., Pittsburgh, PA, 2003.

(17) Scheiner, S.; Kar, T. *J. Phys. Chem. B* **2002**, *106*, 534.

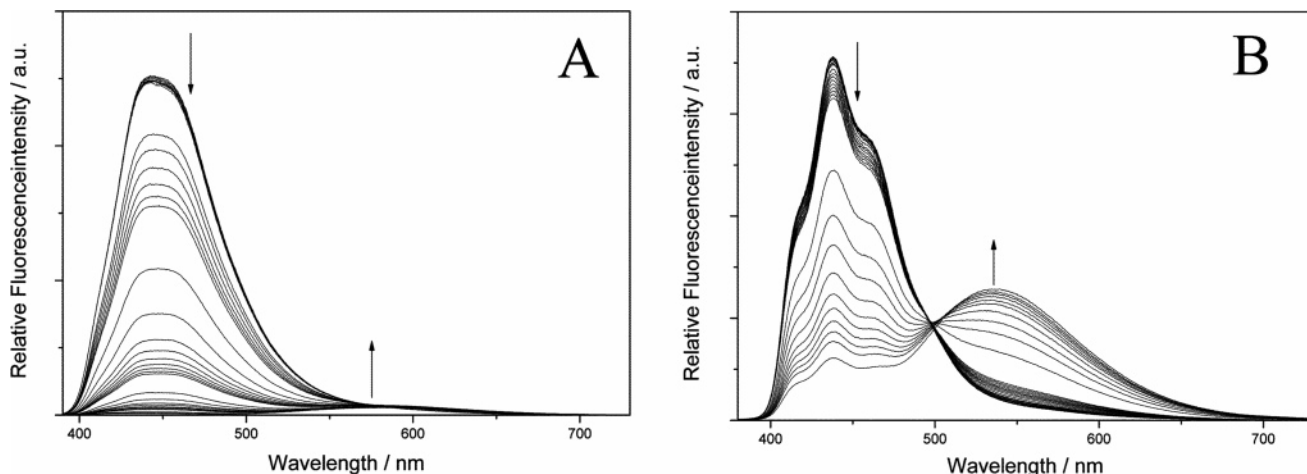


FIGURE 10. (A) Spectrofluorimetric titration of **7** (10^{-5} M in MeOH) with aqueous HCl; arrows indicate the development of band maxima during titration; $\lambda_{\text{ex}} = 370$ nm. Before titration: $c(\text{HCl}) = 0$ M. Titration end: $c(\text{HCl}) = 5.0 \times 10^{-2}$ M. (B) Spectrofluorimetric titration of **7** (10^{-5} M in CHCl_3) with trifluoroacetic acid; arrows indicate the development of band maxima during titration; $\lambda_{\text{ex}} = 370$ nm. Before titration: $c(\text{HCl}) = 0$ M. Titration end: $c(\text{HCl}) = 1.6 \times 10^{-2}$ M.

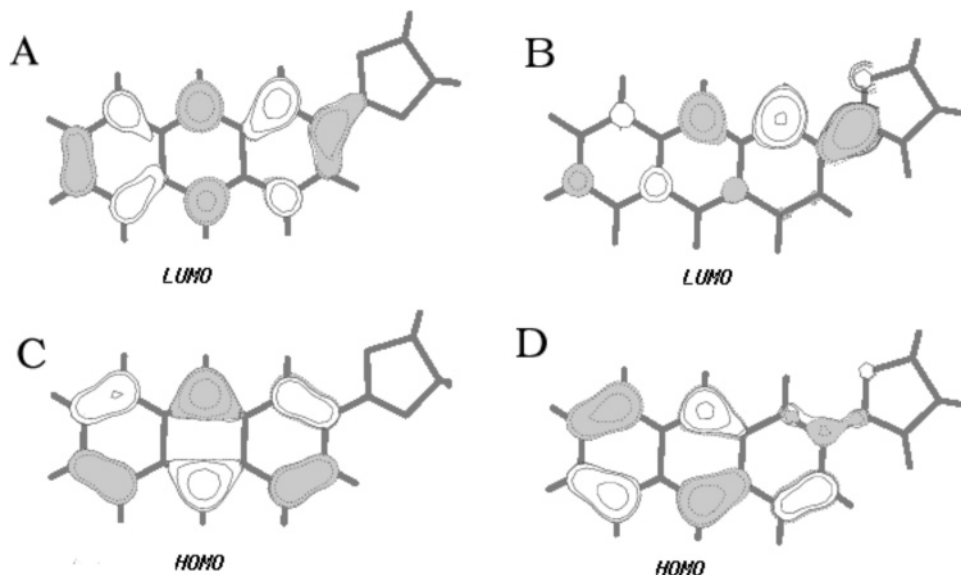


FIGURE 11. Orbital plots (HOMO: C and D, LUMO: A and B) for 2-[2'-(anthryl)]-2-oxazoline **2a'** (A,C) and its *N*-protonated form (B, D); derived from calculations (B3LYP 6-311+G**).

One major drawback of the oxazoline substituent is its limited persistence at low pH due to the acid-catalyzed hydrolysis.¹⁸ Although the initial emission band of the unprotonated oxazoline **2b** may be regained by neutralization, the protonation–neutralization sequence cannot be repeated more than five times, presumably due to substantial decomposition of the oxazoline under these conditions. Thus, we chose the pyridine and benzoxazole moieties, which are stable at lower acid concentrations. Moreover, both heterocycles have already been used as pH-sensitive acceptor substituents in fluorescence probes.^{4c–f} Indeed, the benzoxazole **2c** may be used along these lines, since its absorption and emission properties can also be modified by a change of the acid concentration. Nevertheless, the significantly lower basicity constitutes a notable disadvantage of this system, because **2c** may only be used as an appropriate sensor at

relatively high acid concentrations. In the case of the pyridyl-substituted anthracene **7**, the spectrophotometric acid titration in aqueous solution reveals similar results as in the case of the oxazolines **2a** and **2c**, i.e., a drastic red shift upon protonation of the nitrogen in the heterocyclic moiety of **7** and the accompanying formation of a strong electron acceptor, but the expected red-shifted emission band of its protonated form was not detected in methanol. This observation is in accordance with results obtained with a pyridyl-substituted coumarin derivative, whose fluorescence is also quenched upon protonation without the progression of a corresponding red-shifted fluorescence band.^{3f} However, other pyridyl-substituted fluorophores have been shown to exhibit an intense red-shifted emission in aqueous acids.^{4a,19} Thus, the question remains why protonated **7** is nonfluorescent

(18) Gant, T. G.; Meyers, A. I. *Tetrahedron* **1994**, *50*, 2297.

(19) (a) Wang, S.-L.; Ho, T.-I. *J. Photochem. Photobiol. A: Chem.* **2000**, *135*, 119. (b) Haroutounian, S. A.; Katzenellenbogen, J. A. *Photochem. Photobiol.* **1988**, *47*, 503.

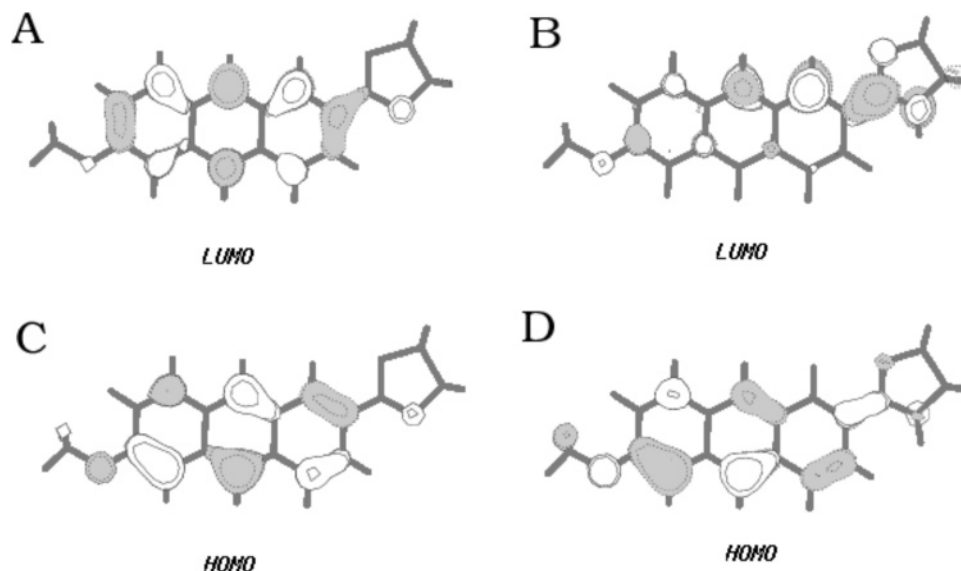


FIGURE 12. Orbital plots (HOMO: C and D, LUMO: A and B) for 2-[2'-(6'-methoxyanthryl)]-2-oxazoline and **2b'** (A,C) and its *N*-protonated form (B,D); derived from calculations (B3LYP 6-311+G**).

in methanol solution. Although it may be suggested that in protonated **7** an excited-state proton transfer from the pyridinium to the solvent takes place, it appears to be unlikely since pyridines usually exhibit larger basicity in the excited state than in the ground state. Quenching processes between ground- and excited-state molecules of the fluorophore can also be excluded since the emission spectrum does not change upon dilution from 10^{-5} to 10^{-6} M. One possibility for the fluorescence quenching in methanol may be the photoinduced intramolecular electron transfer from the anthracene moiety to the pyridinium acceptor, which has been proposed also for pyridinium-substituted 9-vinylanthracene.¹⁴ This PET reaction, which is more likely to take place in the polar solvent methanol than in nonpolar ones, may lead to an intermediate which is radiationless deactivated by the interaction with the solvent (proton transfer or electron transfer) or by a fast electron back transfer. The latter would correspond to a twisted intramolecular charge transfer (TICT) state.²⁰ Since the starting material is already ionic, this phenomenon is usually called a photoinduced charge shift (CS), which is often observed to produce nonemissive excited intermediates in cationic dyes.¹⁴ This explanation of the radiationless deactivation of protonated **7** in methanol is in agreement with the observation that in the nonpolar chloroform emission of **7** is observed upon acidification.

In summary, we investigated the ability of three different *N*-heterocycles to act as acid-sensitive acceptor functionalities in fluorescence probes. All of these heterocycles may be used for such purposes since the protonation of the corresponding fluorogenic probes results in a significant red shift of the emission maxima. In the case of the oxazoline substituent it was shown that its protonated form is such a strong acceptor that even the anthracene without further donor substituents is a sufficient donor to establish an ICT upon light absorption. The benzoxazole and pyridine ring offer a particular

advantage due to their persistence under acidic conditions. Thus, they may be used as efficient fluorescence switches. Nevertheless, the switching of benzoxazole **2c** requires relatively strong acidic conditions, and the pyridine–pyridinium emission switch does not work in aqueous or alcoholic solution. Thus, these systems are not appropriate for applications in analytical biology or medicine. The oxazoline does not exhibit either of these disadvantages, but it is not persistent under permanent acidic conditions. Nevertheless, for a one-time analysis, this system may be very useful. The oxazolines may be protonated in a pH range between 4 and 5 which is very close to physiologically relevant range. Even more important, simple donor-substitution may enhance its basicity, so that proton concentrations of about 6 may be monitored by its emission properties. This is a rather important pH range since tumor tissue usually exhibits similar proton concentrations (pH 6.2–6.6),²¹ as opposed to healthy tissue which is usually neutral (pH 7.5). Further studies directed toward these applications are currently under investigation in our laboratory.

Experimental Section

¹H NMR: 200 and 400 MHz. ¹³C NMR: 50.3 and 101 MHz. C_q, CH, CH₂, and CH₃ were determined by the DEPT pulse sequence. ¹H NMR chemical shifts refer to $\delta_{\text{TMS}} = 0.0$. ¹³C NMR chemical shifts refer to solvent signals (DMSO-*d*₆: $\delta = 39.5$; CD₃CN: $\delta = 1.3, 118.1$). Melting points are uncorrected. Absorption and emission spectra were recorded in deoxygenated spectral grade solvents. Unless noted otherwise, the solution concentrations were 10^{-4} M for absorption spectroscopy and 10^{-5} M for fluorescence spectroscopy. The relative fluorescence quantum yields were determined by the standard method²² with quinine sulfate in 1 N H₂SO₄ as reference ($\phi_{\text{FI}} = 0.546$ ²³). The Britton–Robinson buffer solutions were made

(20) Grabowski, Z. R.; Rotkiewicz, K.; Rettig, W. *Chem. Rev.* **2003**, *103*, 3899.

(21) (a) Stubbs, M.; McSheehy, P. M.; Griffiths, J. R.; Bashford, C. L. *Mol. Med. Today* **2000**, *6*, 15. (b) Smith, C. A.; Sutherland-Smith, A. J.; Keppler, B. K.; Kratz, F.; Baker, E. N. *J. Biol. Inorg. Chem.* **1996**, *1*, 424.

(22) Demas, J. N.; Crosby, G. A. Crosby, *J. Phys. Chem.* **1971**, *75*, 991.

(23) Eaton, D. F. *Pure Appl. Chem.* **1988**, *60*, 1108.

according to literature procedure.²⁴ Because of its low solubility in aqueous solution, the anthracene **2b** was dissolved in DMSO ($c(\mathbf{2b}) = 10^{-4}$ M) and subsequently added to the buffer solutions, so that the buffer also contained 1 vol % of DMSO.

The pK_a data for the ground and excited state (see Table 2) were determined from spectrophotometric titrations according to literature procedures.²⁵

2-[2'-(Anthryl)]-4,4-dimethyl-2-oxazoline (2a). A solution of 383 mg (1.72 mmol) of 2-anthracenecarboxylic acid in 10 mL of oxalyl chloride was heated at reflux for 18 h under argon-gas atmosphere. After evaporation of excess oxalyl chloride in a vacuum, the solid was dissolved in dichloromethane and added dropwise to a solution of 307 mg (3.44 mmol) of 2-amino-2-methylpropanol in 8 mL of dichloromethane at 0 °C. After being for 2 h at 20 °C, the precipitated solid was filtered off. To the remaining solution was added 0.5 mL of thionyl chloride, the solution was kept at reflux for 2 h under argon-gas atmosphere, and after that the solvent was evaporated in a vacuum. The remaining brown solid was washed with diethyl ether. To the solid were added water, diethyl ether, and diluted aqueous NaOH until a pH of 8–9 was indicated. The aqueous phase was extracted twice with diethyl ether, the combined organic phases were dried with $MgSO_4$, and the solvent was removed in a vacuum. Crystallization from *n*-hexane/dichloromethane gave 170 mg (0.62 mmol, 36%) of oxazoline **2a** as a yellow solid. For further purification column chromatography (SiO_2 , *n*-hexane/ethyl acetate 1:1 with 1% pyridine, $R_f = 0.70$) or sublimation (100 °C, 0.4 mbar) was used. Mp: 107–110 °C dec. 1H NMR ($CDCl_3$, 200 MHz): δ 1.45 (s, 6 H, 2 CH_3), 4.20 (s, 2 H, CH_2), 7.47–7.52 (m, 2 H, Ar-H), 8.00–8.04 (m, 4 H, Ar-H), 8.43 (s, 1 H, Ar-H), 8.52 (s, 1 H, Ar-H), 8.69 (s, 1 H, Ar-H). ^{13}C NMR ($CDCl_3$, 100 MHz): δ 28.5 (2 CH_3), 67.7 (C_q), 79.2 (CH_2), 124.1 (CH), 125.7 (CH), 126.2 (CH), 127.2 (CH), 127.4 (CH), 127.9 (CH), 128.2 (CH), 128.4 (CH), 129.4 (CH), 130.7 (C_q), 132.0 (C_q), 132.1 (C_q), 132.6 (C_q), 162.3 (C_q). MS (EI, 70 eV) m/z : 275 (78) [M^+], 260 (100). HRMS: calcd for $C_{19}H_{17}NO$ (275.1310), found 275.1311.

2-[2-(6-Methoxyanthryl)]-4,4-dimethyl-2-oxazoline (2b). A solution of 38.0 mg (0.15 mmol) of 6-methoxy-2-anthracenecarboxylic acid in 3.8 mL of oxalyl chloride was heated at reflux for 18 h under argon-gas atmosphere. After evaporation of excess oxalyl chloride in a vacuum, the solid was dissolved in dichloromethane and added dropwise to a solution of 27.0 mg (0.30 mmol) of 2-amino-2-methylpropanol in 3.8 mL of dichloromethane at 0 °C. After the mixture was stirred for 2 h at 20 °C, the precipitated solid was filtered off. To the remaining solution was added 0.1 mL of thionyl chloride, the solution was kept at reflux for 2 h under argon-gas atmosphere, and after that the solvent was evaporated in a vacuum. The remaining brown solid was washed with diethyl ether. To the solid were added water, diethyl ether, and diluted aqueous NaOH until a pH of 8–9 was indicated. The aqueous phase was extracted twice with diethyl ether, the combined organic phases were dried with $MgSO_4$, and the solvent was removed in a vacuum. Crystallization from *n*-hexane/dichloromethane gave 25.0 mg (0.09 mmol, 60%) of oxazoline **1f** as yellow solid. Mp: 220–225 °C. 1H NMR ($CDCl_3$, 200 MHz): δ 1.44 (s, 6 H), 3.96 (s, 3 H), 4.18 (s, 2 H), 7.14–7.19 (m, 2 H), 7.87–8.01 (m, 3 H), 8.24 (s, 1 H), 8.38 (s, 1 H), 8.55 (s, 1 H). ^{13}C NMR ($CDCl_3$, 50 MHz): δ 28.5 (2 \times CH_3), 55.3 (CH_3), 67.7 (C_q), 79.2 (CH_2), 103.6 (CH), 120.9 (CH), 123.8 (C_q), 124.1 (CH), 124.3 (CH), 127.7 (CH), 127.8 (CH), 128.5 (C_q), 129.3 (C_q), 129.5 (CH), 130.0 (CH), 132.6 (C_q), 133.8 (C_q), 157.8 (C_q), 162.3 (C_q). MS (70 eV, EI) m/z : 305 (82) [M^+], 290 (100), 233 (71), 219 (5), 207 (9), 176 (4), 164 (21). HRMS: calcd for $C_{20}H_{19}N_1O_2$ (305.1416), found 305.1416.

2-[2-(6-Methoxyanthryl)]benzoxazole (2c). Under argon-gas atmosphere, a solution of **1b** (195 mg, 0.77 mmol) in oxalyl

chloride (19.5 mL) was stirred under reflux for 18 h. After evaporation of excess oxalyl chloride in a vacuum, the solid was added to a solution of 2-aminophenol (88.0 mg, 0.80 mmol) in pyridine (2 mL). The solution was stirred for 1 h at 100 °C. The pyridine was evaporated, and the remaining dark residue was heated for 0.5 h at 200 °C under argon-gas atmosphere. Purification by column chromatography (SiO_2 , *n*-hexane/ethyl acetate 6:1, $R_f = 0.31$) and crystallization from *n*-hexane/dichloromethane gave **2c** (84.0 mg, 0.26 mmol, 34%) as a yellow solid. Mp: 148–149 °C. 1H NMR ($CDCl_3$, 200 MHz): δ 3.98 (s, 3 H, OCH_3), 7.17–7.22 (m, 2 H, Ar-H), 7.34–7.42 (m, 2 H, Ar-H), 7.59–7.66 (m, 1 H, Ar-H), 7.78–7.87 (m, 1 H, Ar-H), 7.94 (d, $J = 9.8$ Hz, 1 H, Ar-H), 8.05 (d, $J = 9.0$ Hz, 1 H, Ar-H), 8.23–8.29 (m, 2 H, Ar-H), 8.48 (s, 1 H, Ar-H), 8.91 (s, 1 H, Ar-H). ^{13}C NMR ($CDCl_3$, 50 MHz): δ 55.4 (CH_3), 103.7 (CH), 110.6 (CH), 119.9 (CH), 121.2 (CH), 122.8 (C_q), 123.2 (CH), 124.3 (CH), 124.6 (CH), 125.1 (CH), 128.0 (CH), 128.5 (CH), 128.8 (C_q), 129.1 (CH), 129.4 (C_q), 130.1 (CH), 132.7 (C_q), 134.1 (C_q), 142.2 (C_q), 150.8 (C_q), 158.0 (C_q), 163.4 (C_q). MS (70 eV, EI) m/z : 325 (100) [M^+], 282 (87), 190 (21), 164 (24). Anal. Calcd for $C_{22}H_{15}N_1O_2 \cdot 0.5H_2O$: C, 79.03; H, 4.82; N, 4.19. Found: C, 79.10; H, 4.85; N, 4.11.

2-[2'-(4''-(2'''-Pyridyl)phenyl)hydroxymethyl-4'-methoxyphenyl]-4,4-dimethyl-2-oxazoline (4). To a cooled solution (0 °C) of **3'** (1.02 g, 5.00 mmol) in dry diethyl ether (50 mL) was added *n*-butyllithium (7 mL, 1.6 M in hexane, 5.46 mmol). The solution was stirred for 4 h at 0 °C, and the color changed from yellow to orange and eventually to brown. A solution of (2-pyridyl)benzaldehyde (1.00 g, 5.46 mmol) in diethyl ether (20 mL) was added at 0 °C, and a yellow solid precipitated. The ice bath was removed, and the suspension was stirred for 16 h at rt and subsequently poured into a saturated aqueous solution of NH_4Cl (50 mL). After 15 min of thorough stirring, the aqueous layer was separated and extracted with diethyl ether (20 mL). The combined organic phases were washed with water (30 mL) and dried with $MgSO_4$. After removal of the solvent in a vacuum, **4** was obtained as a yellow solid (2.08 g, >97%) which was spectroscopically pure by 1H NMR. Mp: 102–103 °C. 1H NMR ($CDCl_3$, 400 MHz): δ 1.04 (s, 3 H, CH_3), 1.34 (s, 3 H, CH_3), 3.78 (s, 3 H, OCH_3), 3.92 (d, $J = 8$ Hz, 1 H, CH_2), 3.99 (d, $J = 8$ Hz, 1 H, CH_2), 5.94 (s, 1 H, CH), 6.75 (d, $J = 3$ Hz, 1 H, Ar-H), 6.86 (dd, $J = 9$ Hz, $J = 3$ Hz, 1 H, Ar-H), 7.17–7.24 (m, 1 H, Ar-H), 7.44 (d, $J = 8$ Hz, 1 H, Ar-H), 7.72–7.74 (m, 2 H, Ar-H), 7.84 (d, $J = 9$ Hz, 1 H, Ar-H), 7.94 (d, $J = 9$ Hz, 1 H, Ar-H), 8.66–8.70 (m, 1 H, Ar-H). ^{13}C NMR ($CDCl_3$, 101 MHz): δ 27.9 (CH_3), 28.4 (CH_3), 55.3 (CH_3), 67.7 (C_q), 74.9 (CH), 78.6 (CH_2), 112.0 (CH), 116.7 (CH), 118.9 (C_q), 120.4 (CH), 121.9 (CH), 126.3 (2 \times CH), 127.1 (2 \times CH), 132.6 (CH), 136.7 (CH), 137.8 (C_q), 144.2 (C_q), 146.7 (C_q), 149.6 (CH), 157.4 (C_q), 161.8 (C_q), 162.2 (C_q). MS (EI, 70 eV) m/z : 388 (39) [M^+], 317 (100). Anal. Calcd for $C_{24}H_{24}N_2O_3 \cdot 0.5H_2O$ (397.5): C, 72.52; H, 6.34; N, 7.05. Found: C, 72.59; H, 6.40; N, 6.88.

3-[4'-(2''-Pyridyl)phenyl]-5-methoxyphthalide (5). A solution of **4** (2.08 g, 5.35 mmol) and *p*-toluenesulfonic acid (4.78 g, 25.2 mmol) in toluene (150 mL) was stirred under reflux for 2.5 h. The brown aqueous layer was separated and extracted three times with toluene (50 mL). The combined organic phases were washed with brine and dried $MgSO_4$. After removal of the solvent in a vacuum, **5** was obtained as a yellow solid (1.05 g, 3.30 mmol, 62%). Mp: 151–152 °C. IR (KBr): $\tilde{\nu}$ 1757 cm^{-1} (C=O). 1H NMR ($CDCl_3$, 400 MHz): δ 3.82 (s, 3 H, OCH_3), 6.36 (s, 1 H, CH), 6.74 (d, $J = 2$ Hz, 1 H, Ar-H), 7.06 (dd, $J = 9$ Hz, $J = 2$ Hz, 1 H, Ar-H), 7.24–7.27 (m, 1 H, Ar-H), 7.39, 8.01 (AA'BB' system, 4 H, Ar-H), 7.71–7.79 (m, 2 H, Ar-H), 7.87 (d, $J = 9$ Hz, 1 H, Ar-H), 8.69 (dd, $J = 5$ Hz, $J = 1$ Hz, 1 H, Ar-H). ^{13}C NMR ($CDCl_3$, 101 MHz): δ 55.9 (CH_3), 81.8 (CH), 106.5 (CH), 117.1 (CH), 117.8 (C_q), 120.7 (CH), 122.5 (CH), 127.2 (CH), 127.4 (2 CH), 127.6 (2 CH), 137.0 (CH), 137.3 (C_q), 140.2 (C_q), 149.7 (CH), 152.5 (C_q), 156.5 (C_q), 165.0 (C_q), 170.2 (C_q). MS (EI, 70 eV) m/z : 317 (100) [M^+]. Anal.

(24) Britton, H. T. S.; Robinson, R. A. *J. Chem. Soc.* **1931**, 458.

(25) Polster, J.; Lachmann H. *Spectrometric Titrations – Analysis of Chemical Equilibria*; VCH: Weinheim, 1989.

Calcd for $C_{20}H_{15}NO_3$ (317.3): C, 75.70; H, 4.76; N, 4.41. Found: C, 75.56; H, 4.98; N, 4.41.

4-Methoxy-2-[(4'-(2'-pyridyl)phenyl)methyl]benzoic Acid (6). Zinc dust (16.0 g, 0.25 mol) was activated by successive treatment with diluted hydrochloric acid, water, and methanol and added to a solution of **5** (1.05 g, 3.31 mmol) in acetic acid (150 mL). The suspension was stirred under reflux for 24 h. The zinc dust was filtered off, and the filtrate was poured into a water/ice mixture. The solution was neutralized with aqueous KOH (10%) and extracted four times with dichloromethane (50 mL). The combined organic phases were washed with brine (20 mL) and dried with $MgSO_4$. After removal of the solvent in a vacuum, **6** was obtained as a pale yellow solid (0.79 g, 2.48 mmol, 75%). Mp: 176–177 °C. IR (KBr): $\tilde{\nu}$ 1700 cm^{-1} (C=O). 1H NMR (CD_2Cl_2 , 400 MHz): δ 3.81 (s, 3 H, OCH_3), 4.48 (s, 2 H, CH_2), 6.78 (d, $J = 3$ Hz, 1 H, Ar-H), 6.83 (dd, $J = 9$ Hz, $J = 3$ Hz, 1 H, Ar-H), 7.23 (ddd, $J = 7$ Hz, $J = 5$ Hz, $J = 1$ Hz, 1 H, Ar-H), 7.27, 7.88 (AA'BB' system, 4 H, Ar-H), 7.70 (ddd, $J = 8$ Hz, $J = 1$ Hz, $J = 1$ Hz, 1 H, Ar-H), 7.75 (ddd, $J = 8$ Hz, $J = 7$ Hz, $J = 2$ Hz, 1 H, Ar-H), 8.06 (d, $J = 9$ Hz, 1 H, Ar-H), 8.68 (ddd, $J = 5$ Hz, $J = 2$ Hz, $J = 1$ Hz, 1 H, Ar-H). ^{13}C NMR (CD_2Cl_2 , 101 MHz): δ 40.0 (CH_2), 55.8 (CH_3), 111.8 (CH), 117.8 (CH), 120.9 (CH), 121.3 (C_q), 122.4 (CH), 127.3 (2 CH), 129.7 (2 CH), 134.5 (CH), 137.3 (C_q), 137.4 (CH), 142.5 (C_q), 146.0 (C_q), 149.8 (CH), 157.6 (C_q), 163.5 (C_q), 170.2 (C_q). MS (EI, 70 eV) m/z : 319 (47) [M^+], 274 (100). Anal. Calcd for $C_{20}H_{17}NO_3 \cdot 0.25H_2O$ (289.9): C, 74.17; H, 5.45; N, 4.32. Found: C, 74.13; H, 5.59; N, 4.28.

2-(6-Methoxyanthracen-2-yl)pyridine (7). Under argon-gas atmosphere, **6** (835 mg, 2.62 mmol) was added to methanesulfonic acid (6 mL) at 90 °C. The solution was stirred at 90 °C for 4 h, and its color changed to a dark green color. The reaction mixture was cooled to room temperature and poured into ice–water (200 mL). The solution was stirred for 30 min and treated with aqueous KOH (10%) until a pH = 10 was indicated. The solution was extracted four times with dichloromethane (100 mL). The combined organic phases were washed with saturated aqueous $NaHCO_3$ (100 mL) and water (100 mL) and subsequently dried with $MgSO_4$. The solvent was removed in a vacuum, and the resulting yellow solid (360 mg) was filtered through silica gel and redissolved in 2-propanol

(30 mL) and methanol (5 mL). Argon gas was bubbled through the solution for 30 min to remove oxygen gas. Solid $NaBH_4$ (677 mg, 17.9 mmol) was added, and the solution was stirred under reflux for 4 d. The reaction mixture was poured on ice–water, and excess $NaBH_4$ was decomposed with concd HCl. The suspension was extracted three times with dichloromethane (50 mL). The combined organic phases were dried with $MgSO_4$, the solvent was removed in a vacuum, and the remaining solid was purified by column chromatography (SiO_2 , PE/acetone 3:1, 1% pyridine, $R_f = 0.52$) to give **7** as a yellow powder (157 mg, 550 μ mol, 21% over both steps). Mp: 231–232 °C. 1H NMR ($CDCl_3$, 400 MHz): δ 3.98 (s, 3 H, OCH_3), 7.17 (dd, $J = 9$ Hz, $J = 2$ Hz, 1 H, Ar-H), 7.21 (d, $J = 3$ Hz, 1 H, Ar-H), 7.27 (dd, $J = 8$ Hz, $J = 5$ Hz, 1 H, Ar-H), 7.28 (dd, $J = 8$ Hz, $J = 2$ Hz, 1 H, Ar-H), 7.82 (ddd, $J = 8$ Hz, $J = 8$ Hz, $J = 2$ Hz, 1 H, Ar-H), 7.90–7.93 (m, 2 H, Ar-H), 8.05 (dd, $J = 9$ Hz, $J = 1$ Hz, 1 H, Ar-H), 8.13 (dd, $J = 9$ Hz, $J = 2$ Hz, 1 H, Ar-H), 8.29 (s, 1 H, Ar-H), 8.45 (s, 1 H, Ar-H), 8.62 (s, 1 H, Ar-H), 8.76 (ddd, $J = 5$ Hz, $J = 2$ Hz, $J = 1$ Hz, 1 H, Ar-H). ^{13}C NMR ($CDCl_3$, 101 MHz): δ 55.3 (CH_3), 103.7 (CH), 120.7 (CH), 122.0 (CH), 124.0 (CH), 124.4 (CH), 126.8 (CH), 127.4 (CH), 128.2 (CH), 128.7 (C_q), 130.0 (CH), 132.2 (C_q), 133.3 (C_q), 135.1 (C_q), 136.9 (CH), 149.7 (CH), 157.4 (C_q), 157.5 (C_q). MS (EI, 70 eV) m/z : 285 (100) [M^+]. Anal. Calcd for $C_{20}H_{15}NO \cdot 0.25H_2O$ (289.9): C, 82.88; H, 5.39; N, 4.83. Found: C, 82.89; H, 5.4; N, 4.76.

Acknowledgment. This paper is dedicated to Prof. Hans-Jörg Deiseroth, University of Siegen, on the occasion of his 60th birthday. This work was generously financed by the Bundesminister für Bildung und Forschung, the Deutsche Forschungsgemeinschaft, the Fonds der Chemischen Industrie, and the Welch Foundation of Houston, TX.

Supporting Information Available: Magnified representations of Figures 2–7, 9, and 10. This material is available free of charge via the Internet at <http://pubs.acs.org>.

JO047841Z